13

Polarimetric atom interferometer

© A.Zh. Muradyan

Institute of Physics, Yerevan State University, Yerevan, Republic of Armenia

e-mail: muradyan@ysu.am

Received August 31, 2024
Revised August 31, 2024
Accepted February 23, 2025

In the currently operating light-pulse atom interferometers, the input wave of an atomic matter is split into two components, which then recombine and interfere at the output ports. The interference determines the probability of which port the atom will be registered at. The angle of a single splitting process is very small, and therefore the deflection process is repeated many times. In addition, due to the probabilistic nature of detecting an atom at a particular port, the measurement process must be repeated many times under identical initial conditions. In this paper, a new type of atomic interferometer is proposed, in which the traditional method of measuring the state of an atom is replaced by a highly sensitive method of polarization spectroscopy using the working substance of a clot of atomic condensate. As a result, the proposed design frees the interferometer from the need for the above-mentioned multiple repetitions, while maintaining a high level of sensitivity. Kapitza-Dirac resonance diffraction is used to split the translational motion of an atom. Numerical calculations for determining the rotated component of the probing field show that the ratio of the output signal to the input signal under usual conditions of a specialized laser physics laboratory using a bunch of alkali metal atomic condensate with a concentration of 10^{10} cm^{-3} and linear dimensions of about 10 μm reaches a value of 0.1.

Keywords: atom interferometer, polarization spectroscopy, atomic condensate, Kapitza–Dirac diffraction.

DOI: 10.61011/EOS.2025.04.61415.7036-24

Introduction

A light-pulse atomic interferometer [1–6] is an advanced instrument of quantum metrology and quantum probing [7–9] that relies on the wave nature of matter. Just as in common optical interferometers, an atomic wave packet is split in it into two paths, which are then reflected and recombined. The splitting angle is formed here via Raman photon scattering. Therefore, it is very small and needs to be increased through careful accumulation of numerous (up to several hundred) interaction events [10,11].

The detection method is another aspect that distinguishes an atomic interferometer qualitatively from traditional ones. Drawing directly from the standard quantum measurement theory [12–14], experimenters determine the phase difference here by counting the atoms detected at their ground and excited internal energy levels (output ports). The probabilistic nature of such measurements necessitates multiple repetitions of the entire interaction cycle under identical initial conditions.

A new atomic interferometer design presented below differs form the earlier ones in that the output state of an atom is determined not by counting atoms at two output ports of the interferometer with multiple repetition, but in a single act of highly sensitive polarization spectroscopy of the probing field [15–17]. Another feature of the proposed design is that the interference of atomic waves is established not due to the spatial overlap of two previously separated trajectories, but due to optical transitions between two discrete families of momentum states of translational motion of an atom at its ground and excited internal states generated by Kapitsa–Dirac diffraction.

The first stage of operation of this interferometer is the generation of a family of equidistant momentum states via diffraction of an atom by the resonant field of a standing wave of laser radiation. To this end, the well-known Raman–Nath approximation is extended to longer interaction times, populating the ground and excited internal states of the atom almost equally. At the second stage of interaction, a traveling wave induces interference between the families of momentum states of the ground and excited internal states of the atom. The momentum distributions at the lower and upper internal levels oscillate periodically in the course of this interaction, shifting the distribution centers in opposite directions. The subsequent probing field propagates along the direction of standing and traveling waves, interacts with the atomic ensemble, and projects its states onto the spectrum of rotation of the polarization plane of the probing field. The sought information on residual interference of matter waves is presented in it in the form of an asymmetrically distributed family of narrow maxima that are shifted relative to each other due to the Doppler effect. The use of this diagnostic method should make it possible to simplify significantly the hardware design of the atomic interferometer while preserving its high accuracy.

1. Generation and interference of momentum states of an atom

1.1. Generation of momentum states of an atom by the laser standing-wave field

Consider a two-level atom with mass M and optical transition frequency ω_0 interacting with a laser standing wave with resonant frequency $\omega = \omega_0$ and electric field strength E. The evolution equations for this system are well known and may be written as

$$\left(i\frac{\partial}{\partial t} + \frac{\hbar}{2M}\frac{\partial^2}{\partial z^2}\right) g(z,t) = -2\xi \cos kz\, e(z,t), \qquad (1a)$$

$$\left(i\frac{\partial}{\partial t} + \frac{\hbar}{2M}\frac{\partial^2}{\partial z^2}\right) e(z,t) = -2\xi \cos kz\, g(z,t), \qquad (1b)$$

where $g(z,t)$ and $e(z,t)$ are the atomic wave function components

$$\psi(z,t) = g(z,t)\varphi_E e^{-iE_g t} + e(z,t)\varphi_e^{-iE_e t},$$

corresponding to the ground and excited internal states, respectively; $\xi = dE/\hbar$ is the Rabi frequency for traveling waves that constitute a standing wave; d is the dipole matrix element of the optical transition; and $k = \omega/c$.

We also assume that the atom was at rest prior to the interaction or had a discrete momentum distribution with a pitch of $\hbar k$:

$$g(z,0) = \sum_{n=-\infty}^{\infty} f_n e^{inkz}, \quad e(z,0) = \sum_{n=-\infty}^{\infty} \bar{f}_n e^{indz}.$$

The general solutions of Eqs. (1a), (1b) may then be sought in the form

$$g(z,t) = \sum_{m,n=-\infty}^{\infty} i^m g_m(n,t) e^{i(m+n)kz - i(m+n)^2\omega_r t},$$

$$e(z,t) = \sum_{m,n=-\infty}^{\infty} i^m e_m(n,t) e^{i(m+n)kz - i(m+n)^2\omega_r t}, \qquad (2)$$

where m and n are the numbers of photon momenta acquired in diffraction by a standing wave and present in the initial state, respectively, and $\omega_r = \hbar k^2/2M$ is the recoil frequency. The Schrödinger equation then yields the following system of differential equations for the wave functions included in expansion (2):

$$\frac{dg_m(n,t)}{dt} = \xi e_{m-1}(n,t) e^{i(2m+2n-1)\omega_r t} - \xi e_{m+1}(n,t) e^{i(2m+2n+1)\omega_r t}, \qquad (3a)$$

$$\frac{de_m(n,t)}{dt} = \xi g_{m-1}(n,t) e^{i(2m+2n-1)\omega_r t} - \xi g_{m+1}(n,t) e^{i(2m+2n+1)\omega_r t}. \qquad (3b)$$

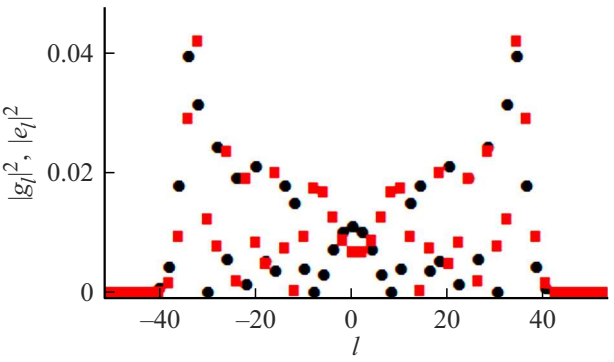

Figure 1. Typical form of the probability distribution of momentum states for the ground (black circles) and excited (red squares) internal states of an atom generated by a standing-wave field.

Substitution $t \to t + 2\pi/\omega$ does not alter these equations; i.e., the sough solutions may be periodic with period $T = 2\pi/\omega_r$.

Owing to the presence of time-dependent exponential coefficients, recurrent system (3a), (3b) does not have exact analytical solutions. The known Raman–Nath approximation [18–20] corresponds to setting the coefficients to unity (i.e., $(2m + 2n \pm 1)\omega, t \ll 1$) and is occasionally called the approximation of short interaction times. We adopt a less stringent interaction time constraint: $\omega_r t \ll 1$. The approximate solutions may then be written as

$$g_m(n,t) = f_n \frac{1 + (-1)^m}{2} e^{i2(m+n)\omega_r t} \times J_m\left(\frac{\xi}{\omega_r(m+n)} \sin(2\omega_r(m+n)t)\right), \qquad (4a)$$

$$e_m(n,t) = f_n \frac{1 - (-1)^m}{2} e^{i2(m+n)\omega_r t} \times J_m\left(\frac{\xi}{\omega_r(m+n)} \sin(2\omega_r(m+n)t)\right), \qquad (4b)$$

where the atom is assumed to remain in the ground state prior to interaction and $J_m(x)$ is the Bessel function. Note that the solution has period $T = 2\pi/\omega_r$. Assuming that the fulfillment of normalization condition

$$\sum_{m,n=-\infty}^{\infty} \left(|g_m(n,t)|^2 + |e_n(n,t)|^2\right) = 1$$

is an indicator of approximation validity, one may easily verify that formulae (4a), (4b) are reliably applicable at $\xi t \le 27$.

It is now possible to rewrite expressions (2) in a more compact form:

$$g(z,t) = \sum_{i=-\infty}^{\infty} g_l(t) e^{ilkzn - il^2\omega_r t},$$

$$e(z,t) = \sum_{i=-\infty}^{\infty} e_l(t) e^{ilkz - il^2\omega_r t} \quad (5)$$

where functions

$$g_1(t) = e^{i2l\omega_r t} \sum_{s=-\infty}^{\infty} i^{\frac{l-s}{2}} f_{\frac{l+s}{2}} \frac{1+(-1)^{\frac{l-s}{2}}}{2} \times J_{\frac{l-s}{2}}\left(\frac{\xi}{\omega_r l}\sin(2\omega_r l t)\right),$$

$$e_1(t) = e^{i2l\omega_r t} \sum_{s=-\infty}^{\infty} i^{\frac{l-s}{2}} f_{\frac{l+s}{2}} \frac{1-(-1)^{\frac{l-s}{2}}}{2} \times J_{\frac{l-s}{2}}\left(\frac{\xi}{\omega_r l}\sin(2\omega_r l t)\right),$$

are the probability amplitudes of l-photon momentum states. They are shown in Fig. 1 (at $\xi = 1.8 \cdot 10^9$ Hz, $t = 10$ ns). It can be seen that the number of momentum states and the approximately unvaried nature of their distribution are quite sufficient for choosing the optimum scenario for subsequent implementation and detection of interference of waves of atomic matter.

2. Formation of asymmetry in the momentum distribution of an atom

Immediately after the generation of momentum states (5), an atom may remain in free motion for a certain time within which

$$g(z,t) = \sum_{l=-\infty}^{\infty} g_l(t_1) e^{ilkz - il^2\omega_r t},$$

$$e(z,t) = \sum_{l=-\infty}^{\infty} e_l(t_1) e^{ilkz - il^2\omega_r z}, \quad (6)$$

where t_1 is the atom–standing wave interaction time. Further interaction (starting from $t_2 \geq t_1$) proceeds between the atom and one of the counter-propagating waves (producing a standing wave). It establishes pairwise mixing of momentum states from the ground and excited levels of the atom, which differ by one photon momentum, and thus induces interference of these matter waves. The resulting amplitudes of the momentum states in the wave function

$$g(z,t) = \sum_{l=-\infty}^{\infty} g_l(t) e^{ilkz},$$

$$e(z,t) = \sum_{l=-\infty}^{\infty} e_l(t) e^{ilkz} \quad (7)$$

are written as

$$g_l(t) = c_{l,1} e^{-i\lambda_{l,1}\omega(t-t_2)} + c_{l,2} e^{-i\lambda_{1,2}\omega_r(t-t_2)},$$

$$e_l(t) = d_{l,1} e^{-i\mu_{i,1}\omega_r(t-t_2)} + d_{l,2} e^{-i\mu_{i,2}\omega_r(t-t_2)}, \quad (8)$$

where

$$c_{l,1} = -\frac{\xi^* e_{l+1}(t_2) + (\lambda_{l,2} - l^2) g_l(t_2)}{\lambda_{l,1} - \lambda_{l,2}},$$

$$c_{l,1} = \frac{\xi^* e_{l+1}(t_2) + (\lambda_{l,1} - l^2) g_l(t_2)}{\lambda_{l,1} - \lambda_{l,2}}, \quad (9)$$

$$d_{l1} = -\frac{\xi g_{l-1}(t_2) + (\mu_{l,2} - l^2) e_l(t_2)}{\mu_{l,1} - \mu_{l,2}},$$

$$d_{l2} = \frac{\xi g_{l-1}(t_2) + (\mu_{l,1} - l^2) e_l(t_2)}{\mu_{l,1} - \mu_{l,2}},$$

$$\lambda_{l,1(2)} = \frac{1}{2} + l + l^2 \mp \sqrt{\frac{1}{4} + l + l^2 + |\xi|^2},$$

$$\mu_{l,1(2)} = \frac{1}{2} - l + l^2 \mp \sqrt{\frac{1}{4} + l + l^2 + |\xi|^2},$$

$$g_l(t_2) = e^{i2l\omega_r t_1 - il^2\omega_r t_2} \sum_{s=-\infty}^{\infty} i^{\frac{l-s}{2}} f_{\frac{l+s}{2}} \times \frac{1+(-1)^{\frac{l-s}{2}}}{2} J_{\frac{l-s}{2}}\left(\frac{\xi}{l}\sin(2\omega_r l t_1)\right),$$

$$g_l(t_2) = e^{i2l\omega_r t_1 - il^2\omega_r t_2} \sum_{s=-\infty}^{\infty} i^{\frac{l-s}{2}} f_{\frac{l+s}{2}} \times \frac{1-(-1)^{\frac{l-s}{2}}}{2} J_{\frac{l-s}{2}}\left(\frac{\xi}{l}\sin(2\omega_r l t_1)\right),$$

and $\xi = \xi/\omega_r$. Formulae (7) and (8) (with the corresponding notation) complete the description of generation and interference of matter waves to be measured at the output of the atomic interferometer.

It should be noted that the resulting momentum distribution features two types of interference. One of them is typical of the problem of scattering by a periodic potential and is represented by the sum over momentum states in the expression of wave function (7). The other is the key dynamic process in the proposed atomic interferometer that is represented by the sums of two terms in the numerators of (9) and mixes the corresponding momentum states of the ground and excited energy levels of the atom.

Polarimetric detection of the result

The polarimetric method may be used to measure state (7) entangled between the translational and internal degrees of freedom of an atom. In this approach, the pump field of the standing and subsequent traveling waves is circularly polarized and couples the magnetic sublevels of a three-level atom (see Fig. 2). It equalizes roughly the populations of the two sublevels and simultaneously forms a discrete set of momentum states, which contain the desired information on interference of waves of atomic matter, at each of them. The probing field has a linear polarization,

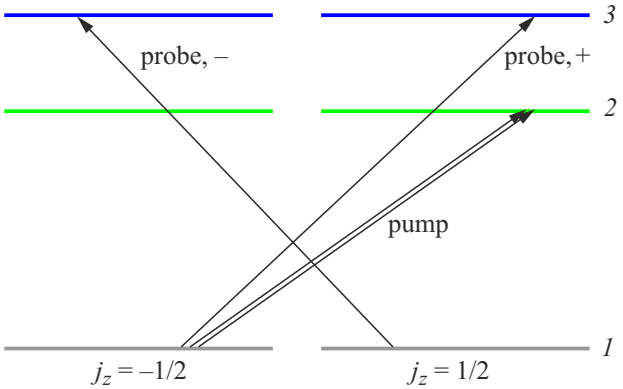

Figure 2. A circularly polarized pump field induces optical anisotropy (in particular, gyrotropy) in the atomic medium (a thin layer of laser-cooled atoms), rotating the plane of polarization of probing radiation.

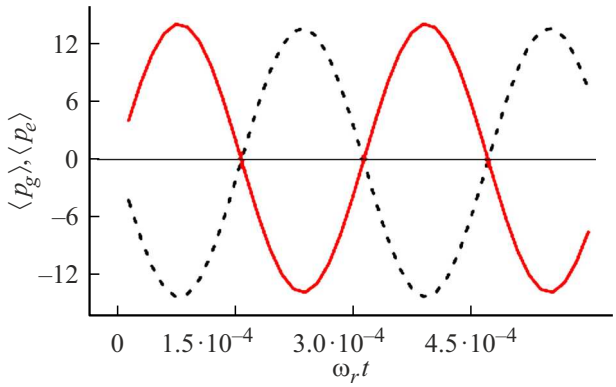

Figure 3. Temporal evolution of the average atomic momentum at the excited (red solid curve) and ground (black dashed curve) internal energy levels of an atom. The momenta are expressed in units of photon recoil momentum. It is assumed that there is no free propagation between the standing and traveling pump waves: $\omega_r t_2 = \omega_r t_1 = \pi 10^{-3}$ and $\xi = 10^4$.

which is represented as the sum of two counter-rotating circular polarizations.

The probing field has a linear polarization, which is represented as the sum of two counter-rotating circular polarizations. The probing field component with the pump field polarization activates optical transition $j_{1,z} = -1/2 \leftrightarrow j_{3,z} = -1/2$, and the reverse polarization activates optical transition $j_{1,z} = 1/2 \pm j_{3,z=-1/2}$ that is not perturbed by the pump field (Fig. 2). Thus, two circular components of the probing wave propagate in the atomic medium with different phase velocities, inducing a rotation of the total linear polarization. In this case, the momentum distribution of the atom (the carrier of information on interference of matter waves) is mapped uniquely due to the Doppler effect onto the frequency spectrum of the rotated probing wave component.

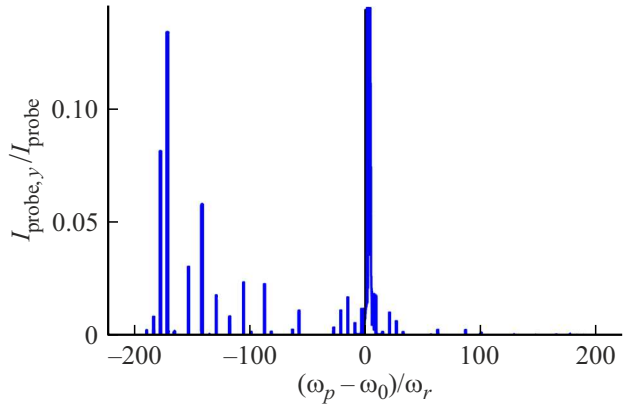

Figure 4. Spectrum of rotated polarization of the probing field at the moment of the first maximum in Fig. 3. Asymmetry is attributable to optical transitions in the running pump field and serves as an indicator of interference of material waves. The resonance detuning of the probing wave is plotted along the horizontal axis in units of recoil frequency ω_r. The thickness and density of the atomic sample are $10\,\mu$m and $10^{10}\,\text{cm}^{-3}$. These values are characteristic of magneto-optical traps. The values of the other parameters are the same as those in Fig. 3.

The mathematical apparatus for calculating the rotating probing field component is well-developed [17] and gives

$$E_{p,y}(z,t) = \frac{E_p(0,t)}{2}\left[\exp(-iq_+F(\omega_p)k_pz) - \exp\left(-i\frac{q}{\Delta_p - k_p\mathbf{v}_r/2 + i\gamma}k_pz\right)\right], \quad (10)$$

where inhomogeneous broadening parameter γ is introduced phenomenologically, $q_\pm = \pi N_\pm |d|^2/3\hbar$, $N_\pm$ — atomic density at sublevels $j_{1,z} = \pm 1/2$, respectively, $k_p = \omega_p/c$, ω_p — circular frequency of the probing wave, d — reduced matrix element of the optical transition, $\Delta_p = \omega_p - \omega_0$, $\mathbf{v}_r = \hbar k/M$ — single-photon recoil velocity, and

$$F(\omega_p) = \sum_{l=-\infty}^{\infty} \frac{|g_l(t_3)|^2}{\Delta_p - 2(l+1/2)k_p\mathbf{v}_r + i\gamma},$$

where t_3 is the moment in time when the running pump wave is switched off.

Naturally, it would be best to optimize and simplify the nature of output signal (10). It is for this purpose that a traveling pump wave was introduced into the interferometer circuit. This wave swings the momentum distributions at the ground and excited levels of the atom in opposite directions with a large amplitude (Fig. 3) [21], creating a Schrödinger cat of sorts in the momentum space. Polarization spectroscopy projects these highly asymmetric momentum distributions onto the spectral distribution of the rotating probing wave component. Figure 4 presents the result in the conditions of the first extremum in Fig. 3.

If it is necessary to have certain preliminary information about the system, the spectrum may be measured immediately after the counter-propagating waves when the atomic momentum distribution is symmetrical with respect to the initial (zero) value.

Summary and conclusions

A new type of atomic interferometer based on well-developed atomic optics and polarization spectroscopy methods was proposed. The dynamic process stage involves the generation of atomic equidistant momentum states via diffraction by a resonant standing electromagnetic wave. Further interference due to interaction with one of the groups of traveling waves swings periodically the momentum distributions at the ground and excited internal energy levels in opposite directions. The measurement stage relies on polarization spectroscopy, wherein the interference pattern of atomic momentum states is reproduced in the spectral distribution of the rotated component of probing electromagnetic radiation.

The conditions under which the atomic interferometer yields optimum and informative measurement results were identified. The conditions established in ordinary specialized laboratories (e.g., atomic cloud density $N = 10^{10}\,\mathrm{cm}^{-3}$ and cloud length $z = 10\,\mu\mathrm{m}$ that were chosen in Fig. 4) are more than sufficient for successful implementation of the proposed atomic interferometer.

It should also be added that, owing to the oscillatory nature of variation of momentum distributions, the spatial displacements of atoms turn out to be smaller than the wavelength of the acting optical fields: atomic trajectories remain completely overlapping at all times. This is indicative of compactness of the polarimetric atomic interferometer design and of the potential appeal of its portable version.

Funding

This study was carried out with financial support of the Higher Education and Science Committee of the Republic of Armenia in the Laboratory for Research and Modeling of Quantum Phenomena of the Institute of Physics of the Yerevan State University.

Conflict of interest

The authors declares that he has no conflict of interest.

References

[1] B.Ya. Dubetskii, A.P. Kazantsev, V.P. Chebotaev, V.P. Yakovlev. Sov. Phys. JETP, **62** (4), 685 (1985).
[2] B.Ya. Dubetskii, A.P. Kazantsev, V.P. Chebotaev, V.P. Yakovlev, JETP Lett., **39** (11), 649 (1984).
[3] Atom Interferometry, ed. by P.R. Berman (Academic Press, San Diego, CA, USA, 1997). DOI: 10.1016/B978-0-12-092460-8.X5000-0
[4] M. Kasevich, S. Chu. Phys. Rev. Lett., **67** (2), 181 (1991). DOI: 10.1103/PhysRevLett.67.181
[5] A.D. Cronin, J. Schmiedmayer, D.E. Pritchard. Rev. Mod. Phys., **81** (3), 1051 (2009). DOI: 10.1103/RevModPhys.81.1051
[6] F.A. Narducci, A.T. Black, J.H. Burke. Adv. Phys. X, **7** (1), 1946426 (2022). DOI: 10.1080/23746149.2021.1946426
[7] L. Pezzé, A. Smerzi, M.K. Oberthaler, R. Schmied, P. Treutlein. Rev. Mod. Phys., **90** (3), 035005 (2018). DOI: 10.1103/RevModPhys.90.035005
[8] C.L. Degen, F. Reinhard, P. Cappellaro. Rev. Mod. Phys., **89** (3), 035002 (2017). DOI: 10.1103/RevModPhys.89.035002
[9] M. Abe, P. Adamson, M. Borcean, D. Bortoletto, K. Bridges, S.P. Carman, S. Chattopadhyay, J. Coleman, N.M. Curfman, K. DeRose et al. Quant. Sci. Technol., **6** (4), 044003 (2021). DOI: 10.1088/2058-9565/abf719
[10] M. Cadoret, E. de Mirandes, P. Clad'e, S. Guellati-Kh'elifa, C. Schwob, F. Nez, L. Julien, F. Biraben. Phys. Rev. Lett., **101** (23), 230801 (2008). DOI: 10.1103/PhysRevLett.101.230801
[11] J. Rudolph, T. Wilkason, M. Nantel, H. Swan, C.M. Holland, Y. Jiang, B.E. Garber, S.P. Carman, J.M. Hogan. Phys. Rev. Lett., **124** (8), 083604 (2020). DOI: 10.1103/PhysRevLett.124.083604
[12] J. von Neumann. *Mathematical Foundations of Quantum Mechanics* (Princeton Univ. Press, 1955).
[13] H.M. Wiseman, G.J. Milburn. *Quantum measurement and control* (Cambridge University Press, Cambridge, 2010). DOI: 10.1017/CBO9780511813948
[14] M.G. Ivanov. *Kak ponimat' kvantovuyu mekhaniku* (NITs „Regulyarnaya i khaoticheskaya dinamika," Institut komp'yuternykh issledovanii, Moskva–Izhevsk, 2015) (in Russian).
[15] C. Wieman, T.W. Hänsch. Phys. Rev. Lett., **36** (20), 1170 (1976). DOI: 10.1103/PhysRevLett.36.1170
[16] A.Zh. Muradyan, L.S. Petrosyan. Opt. Spetrosk., **65** (3), 605 (1988).
[17] W. Demtroder. *Basic Concepts and Instrumentation* (Springer, Berlin, Heidelberg, Germany, 1996), § 10.3. DOI: 10.1007/978-3-662-08260-7
[18] M. Born, E. Wolf. *Principles of Optics* (Pergamon, 1970), para. 12.2.7.
[19] V.M. Arutyunyan, A.Zh. Muradyan. Dokl. Akad. Nauk Arm. SSR, **60** (5), 275 (1975).
[20] R.J. Cook, A.F. Bernhardt. Phys. Rev. A, **18** (6), 2533 (1978). DOI: 10.1103/PhysRevA.18.2533
[21] A.Zh. Muradyan, H.I. Haroutyunyan. Phys. Rev. A, **62** (1), 013401 (2000). DOI: 10.1103/PhysRevA.62.013401

Translated by D.Safin